Nonlinear Dyn (2010) 62: 177–193
DOI 10.1007/s11071-010-9708-4

ORIGINAL PAPER

Delayed saturation controller for vibration suppression in a stainless-steel beam

Jian Xu · Kwok Wai Chung · Yan Ying Zhao

Received: 30 August 2007 / Accepted: 23 March 2010 / Published online: 22 April 2010

Abstract This paper considers the effect of time delays on the saturation control of first-mode vibration of a stainless-steel beam. Time delay is commonly caused by measurements of the system states, transport delay, on-line computation, filtering and processing of data, calculating and executing of control forces as required in control processing. The method of multiple scales is employed to obtain the analytical solutions of limit cycles and their stability and to investigate the bifurcations of the system under consideration. *All the predictions from analytical solutions are in agreement with the numerical simulation*. The analytical results show that a delay can change the range of the saturation control, either widening or shrinking the effective frequency bandwidth. Thus, vibration control of a beam can be achieved using an appropriate choice of the delay in a self-feedback signal. From the examples illustrated, this paper provides a positive example that time delay can also be utilized to suppress vibration in systems when time delay cannot be neglected.

J. Xu (✉) · Y.Y. Zhao
School of Aerospace Engineering and Applied Mechanics, Tongji University, Shanghai 200092, China
e-mail: xujian@mail.tongji.edu.cn

K.W. Chung
Department of Mathematics, City University of Hong Kong, Kowloon, Hong Kong

Keywords Time delay · Saturation control · Stainless-steel beam · Single-mode motion · Nonlinear vibration control

1 Introduction

Nonlinearities are responsible for unusual phenomena in the presence of internal or external resonance. In real applications, the vibration of a primary system is often kept below a critical value when the system is subjected to an external excitation. Thus, various types of controllers are developed so as to channel the excess energy from excitation to the slave system in order that vibration in the primary system be suppressed. One of the novel methods for vibration control is taking advantage of the saturation phenomenon, which is observable in the forced vibrations of coupled two-degree-of-freedom systems with modal interaction. This is because the saturation controller has its attractive feature. With the primary resonance occurring in the system and the amplitude of the forcing term increasing beyond a critical value, the saturation controller can produce a large-amplitude low-frequency response by the internal resonance. Thus, the excess energy from the excitation is absorbed so that the amplitude of the primary system ceases to increase any further and remains constant (saturates). Such energy transfer can ensure that a large-amplitude low-frequency response will not exist in the primary system.

Problems relating to the design of saturation controller have attracted attention for a long time. Haxton and Barr [1] proposed the first passive vibration absorber based on the two-to-one auto-parametric resonance technique. This technique amounts to attaching a cantilever beam with a tip mass to the primary system. When the system is forced at resonance, the absorber could effectively limit the amplitude of the main mass vibration by properly tuning the frequency of the beam. Practically, it is difficult to design an effective passive vibration absorber since the ratio of the internal resonances may not be exactly controlled. In fact, the mechanical controller may induce not only quadratic but also higher order nonlinearities. An efficient alternative for vibration suppression is the active vibration control approach. Nayfeh, Mook and Marshall [2] were first to utilize the saturation phenomenon when analyzing the coupling between the roll and pitch motions of ships. They suppressed successfully the vibration of the system for a wide range of frequencies. When the amplitude of excitation is increased beyond a critical value, the response amplitude of the primary system is saturated at a specific value. Excess energy from excitation is channeled to the second slave system due to the switching of internal resonances. Later, the saturation phenomenon was demonstrated experimentally by Haddow et al. [3], Nayfeh and Zavodney [4], Nayfeh and Balachandran [5], and Oueini et al. [6]. Some practical controllers developed through this strategy include analog electric-circuit controller [7], digital signal [8], piezoelectric patches [9] and Terfenol-D [10]. A so-called saturation control method [9, 11] was used to suppress steady-state vibrations of a dynamical system by connecting it to a second-order controller with quadratic position coupling terms. Recently, Pratt et al. [12] designed a refined nonlinear vibration controller by using a quadratic velocity coupling term in the controller and adding a negative velocity feedback to the system. They employed the saturation phenomenon and internal resonance conditions to control the transient and first-mode steady-state vibrations of a cantilever beam using PZT patches as actuators and sensors. Sagurarum et al. [13] used numerical simulations to demonstrate how full modal coupling, due to the presence of piezoelectric actuators, affects the response and performance of a saturation controller applied to a uniform cantilever beam. Their results suggested that the modal coupling had a significant effect on the beam response, which was not present when modal coupling was neglected. In [14], Shoeybi and Ghorashi considered a plant consisting of a Permanent Magnet Direct Current (PMDC) motor and introduced a second-order nonlinear controller with a quadratic control law, resulting in a two-degree-of-freedom system. The singular point analysis was used in order to study the local stability of the steady-state solutions. It was shown that the closed-loop system exhibited different stability regimes. Then, Shoeybi and Ghorashi [15] extended their research to consider the effect of dry friction on the response and stability of a system with an active vibration absorber operating on the basis of utilizing the saturation phenomenon. Based on the saturation phenomenon associated with the dynamical systems with quadratic nonlinearities and a two-to-one internal resonance, Li et al. [16] considered the effect of active vibration control on a nonlinear plant subjected to primary excitation. Their results show that the control scheme possesses a wide suppression bandwidth once the frequency of the absorber is properly tuned.

For an active control system, all operations in the control process are not instantaneous, which implies that various delays exist inevitably in the real-time control performance. In fact, these delays may be caused by measurements of the system states, physical properties of the equipment applied for control, transport delay, on-line computation, filtering and processing of data, calculating and executing of the control forces as required in control processing. The goal of vibration control may not be realized if the delay in the controlled system is neglected. Thus, the effect of time delays on a controller should be taken into consideration since they cannot be eliminated even with the most updated technology [17–20]. On the one hand, our previous research [21] showed that various delays could induce instability of a system. It is necessary to determine the maximum allowable delay value, which maintains a stable system. Sometimes, control gains are compensated for overcoming this defect. Guan [22] studied a gearbox system with time delay. In order to improve the vibration reduction performance of the control system, the technique of delay compensation was employed. On the other hand, the time delay has its advantages. It may be used as a "switch" to control the resonance stability and the amplitude peak [23, 24]. Furthermore, the time delay is utilized in the so-called delayed resonator [25, 26] to remove the linear vibration of a primary system. The delayed

resonator is easy to implement and only requires one feedback from the system. However, its operational frequency is bounded due to the linear absorber. Thus, Zhao and Xu [27] designed a device which was composed of a delayed resonator and a nonlinear vibration absorber for the nonlinear vibration suppression of a two-degree-of-freedom system. This technique offers a number of attractive advantages in eliminating vibrations of a primary system, such as tuning in real time, wide range of frequencies, perfect total suppression and simplicity of the control.

In summary, it is essential to consider the effect of time delays, which exist in a controlled system, on vibration suppression or saturation control. To this end, a popular controlled system presented in [12] is chosen as the model of this paper for the convenience of comparison. The time delays will be chosen as the variable parameters. As a result, it is demonstrated that the range of the saturation control can be varied with the different delays so that the effective frequency bandwidth of the saturation control shrinks or is widened. In the theoretical aspect, this paper also provides the evidence that the delay has positive and negative effect on the saturation control.

2 Background of the model

The following equations describe the first-mode vibration of a cantilever stainless-steel beam together with the saturation controller:

$$\ddot{u}_1 + 2\zeta_1\omega_1\dot{u}_1 + \omega_1^2 u_1 = g_2\dot{u}_1\dot{u}_2, \tag{1}$$

$$\ddot{u}_2 + 2\zeta_2\omega_2\dot{u}_2 + \omega_2^2 u_2 = -2g_3\omega_2\dot{u}_2 + g_1 u_1^2 + F\cos(\Omega t), \tag{2}$$

where u_1 denotes the response of the controller, ω_1 its natural angular frequency, and ζ_1 its damping ratio, u_2 represents the response of the controlled system, ω_2 its natural frequency close to $2\omega_1$ and ζ_2 its damping ratio. Moreover, g_1 and g_2 are positive gain constants, $\dot{u}_1\dot{u}_2$ the feedback signal, u_1^2 the control signal, g_3 the velocity feedback gain, $-2g_3\omega_2\dot{u}_2$ the self-feedback signal, F the positive coefficient of amplitude corresponding to the external excitation force, Ω the frequency of external excitation, t the time, and $(\cdot) \equiv d()/dt$.

In a real-time vibration-suppression control system, delays exist in the feedback, control and self-feedback signals. Obviously, the dynamical behaviors of the system are influenced by these delays. Thus, it is necessary to include delays in the control system as

$$\ddot{u}_1(t) + 2\zeta_1\omega_1\dot{u}_1(t) + \omega_1^2 u_1(t) = g_2\dot{u}_1(t)\dot{u}_2(t-\tau_2), \tag{3}$$

$$\ddot{u}_2(t) + 2\zeta_2\omega_2\dot{u}_2(t) + \omega_2^2 u_2(t) = -2g_3\omega_2\dot{u}_2(t-\tau_3) + g_1 u_1^2(t-\tau_1) + F\cos(\Omega t), \tag{4}$$

where τ_1, τ_2 and τ_3 are the time delays of the control, feedback and self-feedback signals, respectively.

If the delays are taken into consideration in a controlled system, one of the following two possible cases will happen in the system: (i) the first mode is not involved in an internal resonance with any of the other modes or external combination resonance; (ii) the delay induces an internal resonance with the higher vibration modes or external combination resonance. In this paper, we consider only the first case as the main interest usually focuses on the control of the first mode. Therefore, we assume a single-mode dynamics for the beam.

3 Perturbation analysis

In this section, the method of multiple scales is employed in the perturbation analysis. A small dimensionless perturbation parameter ε $(0 < \varepsilon < 1)$ is introduced to the equations for bookkeeping only. A fast scale is characterized by $T_0 = t$ with the motion at Ω and a slow scale by $T_1 = \varepsilon t$. We set $\bar{g}_3 = \varepsilon g_3$, $\xi_1 = \varepsilon\zeta_1$, $\xi_2 = \varepsilon\zeta_2$ and $F = \varepsilon^2 f$ so as to have the damping, nonlinear terms and primary resonance force, respectively, appearing in the same perturbation magnitude. The method of multiple scales is employed to seek a second-order approximate solution of (3) and (4) using the following form:

$$u_1(t,\varepsilon) = \varepsilon u_{11}(T_0,T_1) + \varepsilon^2 u_{12}(T_0,T_1) + \cdots, \tag{5}$$

$$u_2(t,\varepsilon) = \varepsilon u_{21}(T_0,T_1) + \varepsilon^2 u_{22}(T_0,T_1) + \cdots, \tag{6}$$

$$u_{1\tau_1}(t,\varepsilon) = \varepsilon u_{11\tau_1}(T_0,T_1) + \varepsilon^2 u_{12\tau_1}(T_0,T_1) + \cdots, \tag{7}$$

$$u_{2\tau_2}(t,\varepsilon) = \varepsilon u_{21\tau_2}(T_0,T_1) + \varepsilon^2 u_{22\tau_2}(T_0,T_1) + \cdots, \tag{8}$$

$$u_{2\tau_3}(t,\varepsilon) = \varepsilon u_{21\tau_3}(T_0,T_1) + \varepsilon^2 u_{22\tau_3}(T_0,T_1) + \cdots. \quad (9)$$

The derivatives with respect to time are expressed in terms of the new scales as

$$\frac{d}{dt} = D_0 + \varepsilon D_1 + \cdots, \quad (10)$$

$$\frac{d^2}{dt^2} = D_0^2 + 2\varepsilon D_0 D_1 + \cdots, \quad (11)$$

where $D_k = \partial/\partial T_k$, $k = 0, 1$.

Substituting (5)–(11) into (3) and (4), and equating coefficients of like powers of ε yield

Order ε^1:

$$D_0^2 u_{11} + \omega_1^2 u_{11} = 0, \quad (12)$$

$$D_0^2 u_{21} + \omega_2^2 u_{21} = 0. \quad (13)$$

Order ε^2:

$$D_0^2 u_{12} + \omega_1^2 u_{12} = -2D_0 D_1 u_{11} - 2\xi_1\omega_1 D_0 u_{11} + g_2 D_0 u_{11} D_0 u_{21\tau_2}, \quad (14)$$

$$D_0^2 u_{22} + \omega_2^2 u_{22} = -2D_0 D_1 u_{21} - 2\xi_2\omega_2 D_0 u_{21} + g_1 u_{11\tau_1}^2 - 2g_3\omega_2 D_0 u_{21\tau_3} + f\cos\Omega T_0. \quad (15)$$

The solutions of (12) and (13) can be expressed as

$$u_{11} = A_1(T_1)e^{i\omega_1 T_0} + cc, \quad (16)$$

$$u_{21} = A_2(T_1)e^{i\omega_2 T_0} + cc, \quad (17)$$

where A_1 and A_2 are arbitrary functions at this level of approximation, $i \equiv \sqrt{-1}$, and cc denotes the complex conjugate terms. The external excitation may be given by

$$f\cos\Omega T_0 = \frac{1}{2} f e^{i\Omega T_0} + cc. \quad (18)$$

The time delay items can be expressed as

$$u_{11\tau_1} = A_{1\tau_1}(T_1)e^{i\omega_1(T_0-\tau_1)} + cc, \quad (19)$$

$$u_{21\tau_2} = A_{2\tau_2}(T_1)e^{i\omega_2(T_0-\tau_2)} + cc, \quad (20)$$

$$u_{21\tau_3} = A_{2\tau_3}(T_1)e^{i\omega_2(T_0-\tau_3)} + cc. \quad (21)$$

Expanding $A_{1\tau_1}$, $A_{2\tau_2}$ and $A_{2\tau_3}$ into a Taylor series [28] yields

$$A_{1\tau_1} = A_1(T_1 - \varepsilon\tau_1) = A_1(T_1) - \varepsilon\tau_1 A_1'(T_1) + \cdots, \quad (22)$$

$$A_{2\tau_2} = A_2(T_1 - \varepsilon\tau_2) = A_2(T_1) - \varepsilon\tau_2 A_2'(T_1) + \cdots, \quad (23)$$

$$A_{2\tau_3} = A_2(T_1 - \varepsilon\tau_3) = A_2(T_1) - \varepsilon\tau_3 A_2'(T_1) + \cdots. \quad (24)$$

Substituting (16)–(24) into (14) and (15), we obtain

$$D_0^2 u_{12} + \omega_1^2 u_{12} = -g_2\omega_1\omega_2 A_1 A_2 e^{i[(\omega_1+\omega_2)T_0 - \omega_2\tau_2]} + g_2\omega_1\omega_2 \bar{A}_1 A_2 e^{i[(\omega_2-\omega_1)T_0-\omega_2\tau_2]} - 2i\omega_1(A_1' + \xi_1\omega_1 A_1)e^{i\omega_1 T_0} + cc, \quad (25)$$

$$D_0^2 u_{22} + \omega_2^2 u_{22} = g_1 A_1^2 e^{2i\omega_1(T_0-\tau_1)} + g_1 A_1\bar{A}_1 - 2ig_3\omega_2^2 A_2 e^{i\omega_2(T_0-\tau_3)} + \frac{1}{2} f e^{i\Omega T_0} - 2i\omega_2(A_2' + \xi_2\omega_2 A_2)e^{i\omega_2 T_0} + cc, \quad (26)$$

where $()' \equiv \partial()/\partial T_1$. We are going to consider the primary and the 1:2 internal resonances since the controller for these cases may absorb the energy.

To describe the nearness of the internal resonance quantitatively, a detuning parameter σ_1 is introduced as

$$2\omega_1 = \omega_2 + \varepsilon\sigma_1. \quad (27)$$

Similarly, the nearness of the external resonance is represented by a detuning parameter σ_2 defined as

$$\Omega = \omega_2 + \varepsilon\sigma_2. \quad (28)$$

Substituting (27) and (28) into (25) and (25), and setting the coefficients of the secular terms to zero yield the solvability conditions which are given by

$$-2i\omega_1(A_1' + \xi_1\omega_1 A_1) + g_2\omega_1\omega_2\bar{A}_1 A_2 e^{-i(\sigma_1 T_1 + \omega_2\tau_2)} = 0, \quad (29)$$

$$-2i\omega_2(A_2' + \xi_2\omega_2 A_2) - 2ig_3\omega_2^2 A_2 e^{-i\omega_2\tau_3} + g_1 A_1^2 e^{i(\sigma_1 T_1 - 2\omega_1\tau_1)} + \frac{1}{2} f e^{i\sigma_2 T_1} = 0. \quad (30)$$

It follows from (29) and (30) that adding the negative velocity feedback with delay $-2g_3\omega_2\dot{u}_2(t-\tau_3)$ in (4) can improve significantly the effective damping of the system since the internal resonance between the beam and controller can be activated. Hence, it can either facilitate the energy transfer, minimize it, or even completely destabilize the linear system if the resulting damping turns out to be positive. We will also see that the resonant region can be modified since the delay has the effect of phase-shifting.

Introducing the polar notation $A_1(T_1)=\frac{1}{2}a_1(T_1)\times e^{i\theta_1(T_1)}$ and $A_2(T_1)=\frac{1}{2}a_2(T_1)e^{i\theta_2(T_1)}$ into (29) and (30), and setting the coefficients of the real and imaginary parts to zero yield the modulation equations as

$$a_1' = -\omega_1\xi_1 a_1 + \frac{g_2\omega_2}{4}a_1a_2\big[-\cos\phi_1\sin(\omega_2\tau_2) + \sin\phi_1\cos(\omega_2\tau_2)\big], \tag{31}$$

$$a_2' = -\omega_2\big[\xi_2+g_3\cos(\omega_2\tau_3)\big]a_2 - \frac{g_1}{4\omega_2}\big[\cos\phi_1\sin(2\omega_1\tau_1) + \sin\phi_1\cos(2\omega_1\tau_1)\big]a_1^2 + \frac{1}{2\omega_2}f\sin\phi_2, \tag{32}$$

$$\theta_1' a_1 = -\frac{g_2\omega_2}{4}\big[\cos\phi_1\cos(\omega_2\tau_2) + \sin\phi_1\sin(\omega_2\tau_2)\big]a_1a_2, \tag{33}$$

$$\theta_2' a_2 = -\frac{g_1}{4\omega_2}\big[\cos\phi_1\cos(2\omega_1\tau_1) + \sin\phi_1\sin(2\omega_1\tau_1)\big]a_1^2 + g_3\omega_2\sin(\omega_2\tau_3)a_2 - \frac{1}{2\omega_2}f\cos\phi_2, \tag{34}$$

where $\phi_1=\theta_2-2\theta_1-\sigma_1T_1$, $\phi_2=\sigma_2T_1-\theta_2$. Equations (31)–(34) can also be rewritten as

$$a_1' = -\omega_1\xi_1 a_1 + \frac{g_2\omega_2}{4}a_1a_2\big[-\cos\phi_1\sin(\omega_2\tau_2) + \sin\phi_1\cos(\omega_2\tau_2)\big], \tag{35}$$

$$a_2' = -\omega_2\big[\xi_2+g_3\cos(\omega_2\tau_3)\big]a_2 - \frac{g_1}{4\omega_2}\big[\cos\phi_1\sin(2\omega_1\tau_1) + \sin\phi_1\cos(2\omega_1\tau_1)\big]a_1^2 + \frac{1}{2\omega_2}f\sin\phi_2, \tag{36}$$

$$\frac{\phi_1'+\phi_2'}{2}a_1 = \frac{\sigma_2-\sigma_1}{2}a_1 + \frac{g_2\omega_2}{4}\big[\cos\phi_1\cos(\omega_2\tau_2) + \sin\phi_1\sin(\omega_2\tau_2)\big]a_1a_2, \tag{37}$$

$$\phi_2' a_2 = \sigma_2 a_2 + \frac{g_1}{4\omega_2}\big[\cos\phi_1\cos(2\omega_1\tau_1) - \sin\phi_1\sin(2\omega_1\tau_1)\big]a_1^2 - g_3\omega_2\sin(\omega_2\tau_3)a_2 + \frac{1}{2\omega_2}f\cos\phi_2. \tag{38}$$

4 Theoretical analysis of equilibrium solutions

The amplitudes a_1 and a_2 are assumed to be positive here. Equations (35)–(38) may have three possible equilibrium solutions, given by

$$E_1(a_1,a_2) = \left(0, \frac{f}{2\omega_2\sqrt{[\sigma_2-g_3\omega_2\sin(\omega_2\tau_3)]^2+[\xi_2+g_3\cos(\omega_2\tau_3)]^2\omega_2^2}}\right), \tag{39}$$

$$E_2(a_1,a_2) = \left(\sqrt{-b-\sqrt{b^2-c}}, \frac{4}{g_2}\sqrt{\left(\frac{\omega_1}{\omega_2}\xi_1\right)^2+\left(\frac{\sigma_1-\sigma_2}{2\omega_2}\right)^2}\right), \tag{40}$$

$$E_3(a_1,a_2) = \left(\sqrt{-b+\sqrt{b^2-c}}, \frac{4}{g_2}\sqrt{\left(\frac{\omega_1}{\omega_2}\xi_1\right)^2+\left(\frac{\sigma_1-\sigma_2}{2\omega_2}\right)^2}\right), \tag{41}$$

where

$$\begin{aligned} b = \frac{8}{g_1g_2}\Big\{&\big[g_3\omega_2\sin(2\omega_1\tau_1)\cos(\omega_2\tau_3) - g_3\omega_2\cos(2\omega_1\tau_1)\sin(\omega_2\tau_3) + \sin(2\omega_1\tau_1)\xi_2\omega_2 + \sigma_2\cos(2\omega_1\tau_1)\big] \\ &\times\big[(\sigma_1-\sigma_2)\cos(\omega_2\tau_2) - 2\xi_1\omega_1\sin(\omega_2\tau_2)\big] \\ &+\big[g_3\omega_2\cos(2\omega_1\tau_1)\cos(\omega_2\tau_3) + g_3\omega_2\sin(2\omega_1\tau_1)\sin(\omega_2\tau_3) + \xi_2\omega_2\cos(2\omega_1\tau_1) - \sigma_2\sin(2\omega_1\tau_1)\big] \\ &\times\big[2\xi_1\omega_1\cos(\omega_2\tau_2) + (\sigma_1-\sigma_2)\sin(\omega_2\tau_2)\big]\Big\}, \end{aligned} \tag{42}$$

$$c = \left(\frac{16}{g_1 g_2}\right)^2 \{[\sigma_2 - g_3\omega_2 \sin(\omega_2\tau_3)]^2 + \omega_2^2[\xi_2 + g_3\cos(\omega_2\tau_3)]^2\} \times \left[\omega_1^2\xi_1^2 + \frac{1}{4}(\sigma_2 - \sigma_1)^2\right] - \frac{4f^2}{g_1^2}. \tag{43}$$

It is obvious that the equilibrium solution E_1 always exists in (35)–(38). The system is in a single-mode motion if E_1 is unique and stable. The equilibrium solution E_2 or E_3 may occur when E_1 is unstable. Therefore, a coupled-mode motion may occur in the system. Since a_2 is independent of the external amplitude f at E_2 or E_3 when $-b - \sqrt{b^2 - c} > 0$ or $-b + \sqrt{b^2 - c} > 0$ for $b^2 - c > 0$, it follows from (40) and (41) that the vibration of the controlled or primary system (4) is saturated. This implies that the saturation phenomenon occurs if and only if E_2 or E_3 exists. We can easily conclude that if the system has two or three equilibrium solutions, it is in the saturation control state. The existence of E_2 or E_3 depends on the values of b and c. As $c \geq 0$, it follows from (43) that $f \leq F_2$ where F_2 is defined as

$$F_2 = \sqrt{\frac{64}{g_2^2}\{[\sigma_2 - g_3\omega_2\sin(\omega_2\tau_3)]^2 + \omega_2^2[\xi_2 + g_3\cos(\omega_2\tau_3)]^2\}\left[\omega_1^2\xi_1^2 + \frac{1}{4}(\sigma_2 - \sigma_1)^2\right]}. \tag{44}$$

For $b^2 - c \geq 0$, we obtain from (42) and (43) that $f \geq F_1$ where F_1 is defined as

$$F_1 = \frac{\sqrt{4F_2^2 - b^2 g_1^2}}{2}. \tag{45}$$

Next, we consider the conditions of saturation control for the two cases: $b < 0$ and $b \geq 0$. For $b < 0$, E_2 and E_3 may exist which correspond to two different excitation levels: (i) E_1, E_2 and E_3 exist if $F_1 \leq f \leq F_2$; (ii) E_1 and E_3 exist if $f \geq F_2$. For $b \geq 0$, E_1 and E_3 exist if $f > F_2$. Accordingly, the conditions of a single-mode motion are given for $b < 0$ and $b \geq 0$, respectively. For $b < 0$, E_1 exists only if $f < F_1$ (i.e., $b^2 - c < 0$). For $b \geq 0$, the condition for the existence of E_1 only is $f \leq F_2$ (i.e., $c \geq 0$). Similarly, the system is in a single-mode motion when only a single equilibrium solution E_1 exists.

From the above analysis we can conclude that the occurrence of the single-mode motion or the saturation motion depends on the value of external amplitude f. The critical value of f is F_1 for $b < 0$ and F_2 for $b \geq 0$. Since F_1 and F_2 are determined by the time delays τ_1, τ_2 and τ_3, this suggests that both the single-mode motion and the saturation control are influenced by these delays. Thus, it is necessary to analyze the stability of the equilibrium solutions and the effect of the delays on the saturation control of the system.

5 Stability of equilibrium solutions

The equilibrium solutions in (39)–(41) correspond to the steady-state solutions of (35)–(38). To determine their stability, we introduce the Cartesian coordinates (p_1, p_2, q_1, q_2) as

$$p_1 = a_1\cos\phi_1, \qquad q_1 = a_1\sin\phi_1, \qquad p_2 = a_2\cos(\phi_1 + \phi_2), \qquad q_2 = a_2\sin(\phi_1 + \phi_2). \tag{46}$$

Using (46), we transform (35)–(38) into

$$p_1' = -\omega_1\xi_1 p_1 - \frac{1}{2}(\sigma_2 - \sigma_1)q_1 - \frac{1}{4}g_2\omega_2\sin(\omega_2\tau_2)(p_1p_2 + q_1q_2) + \frac{1}{4}g_2\omega_2\cos(\omega_2\tau_2)(q_1p_2 - p_1q_2), \tag{47}$$

$$q_1' = -\omega_1\xi_1 q_1 + \frac{1}{2}(\sigma_2 - \sigma_1)p_1 + \frac{1}{4}g_2\omega_2\sin(\omega_2\tau_2)(q_1p_2 - p_1q_2) + \frac{1}{4}g_2\omega_2\cos(\omega_2\tau_2)(p_1p_2 + q_1q_2), \tag{48}$$

$$p_2' = -\omega_2\xi_2 p_2 - \sigma_2 q_2 + \frac{1}{4\omega_2}g_1\sin(2\omega_1\tau_1)\left(q_1^2 - p_1^2\right)$$

$$
\begin{aligned}
&- \frac{1}{2\omega_2} g_1 \cos(2\omega_1 \tau_1) \\
&+ g_3 \omega_2 \big[\sin(\omega_2 \tau_3) q_2 - \cos(\omega_2 \tau_3) p_2\big], \qquad (49)
\end{aligned}
$$

$$
\begin{aligned}
q_2' = &-\omega_2 \xi_2 q_2 + \sigma_2 p_2 \\
&- \frac{1}{2\omega_2} g_1 \sin(2\omega_1 \tau_1) p_1 q_1 \\
&+ \frac{1}{4\omega_2} g_1 \cos(2\omega_1 \tau_1)\big(p_1^2 - q_1^2\big) \\
&- g_3 \omega_2 \big[\sin(\omega_2 \tau_3) p_2 + \cos(\omega_2 \tau_3) q_2\big]. \qquad (50)
\end{aligned}
$$

Equations (47)–(50) are perturbed by a small perturbation to determine the stability of the equilibrium solutions. The perturbation equations are shown as

$$
\begin{aligned}
&\big\{\Delta p_1', \Delta q_1', \Delta p_2', \Delta q_2'\big\}^{\mathrm{T}} \\
&\quad = [J]\{\Delta p_1, \Delta q_1, \Delta p_2, \Delta q_2\}^{\mathrm{T}}, \qquad (51)
\end{aligned}
$$

where T denotes transpose of the matrix and $[J]$ is the Jacobian matrix. The characteristic equation corresponding to a fixed equilibrium solution may be expressed as

$$
\lambda^4 + \delta_1 \lambda^3 + \delta_2 \lambda^2 + \delta_3 \lambda + \delta_4 = 0, \qquad (52)
$$

where λ denotes eigenvalues of $[J]$ and δ_1, δ_2, δ_3 and δ_4 are coefficients of the equation. The equilibrium so-

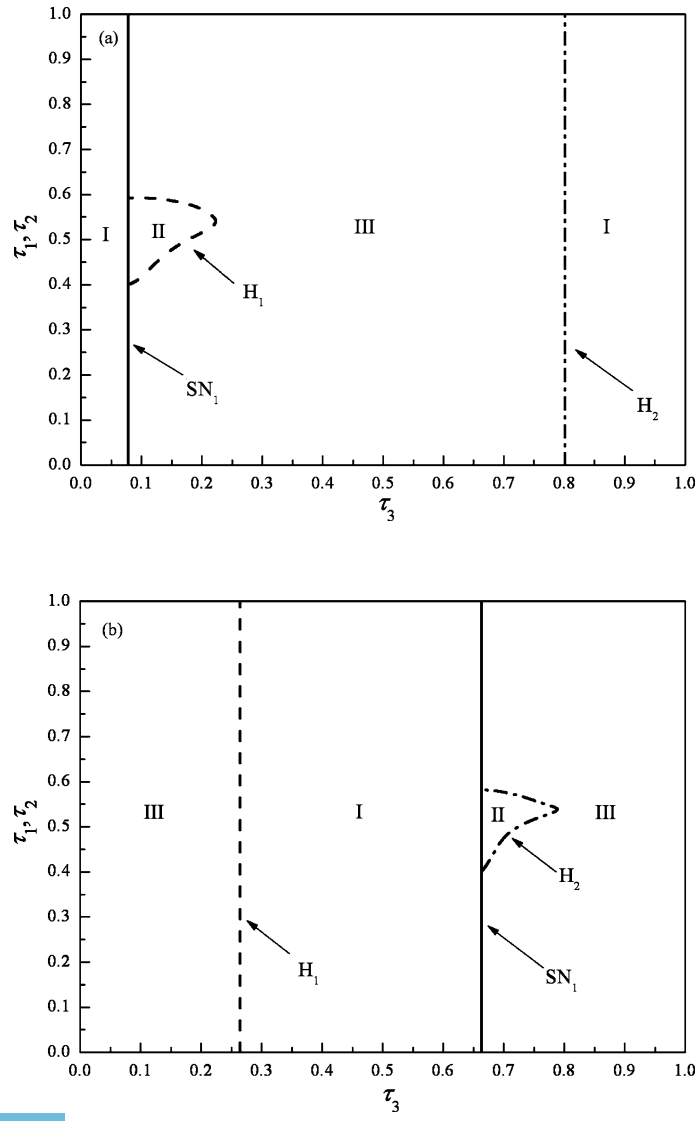

Fig. 1 Analytical prediction for single mode (I), saturation (II) and complex vibrations (III) in (3) and (4): (**a**) $\sigma_2 = 0.5$, $g_3 = 0.10$; (**b**) $\sigma_2 = 0.6$, $g_3 = -0.10$

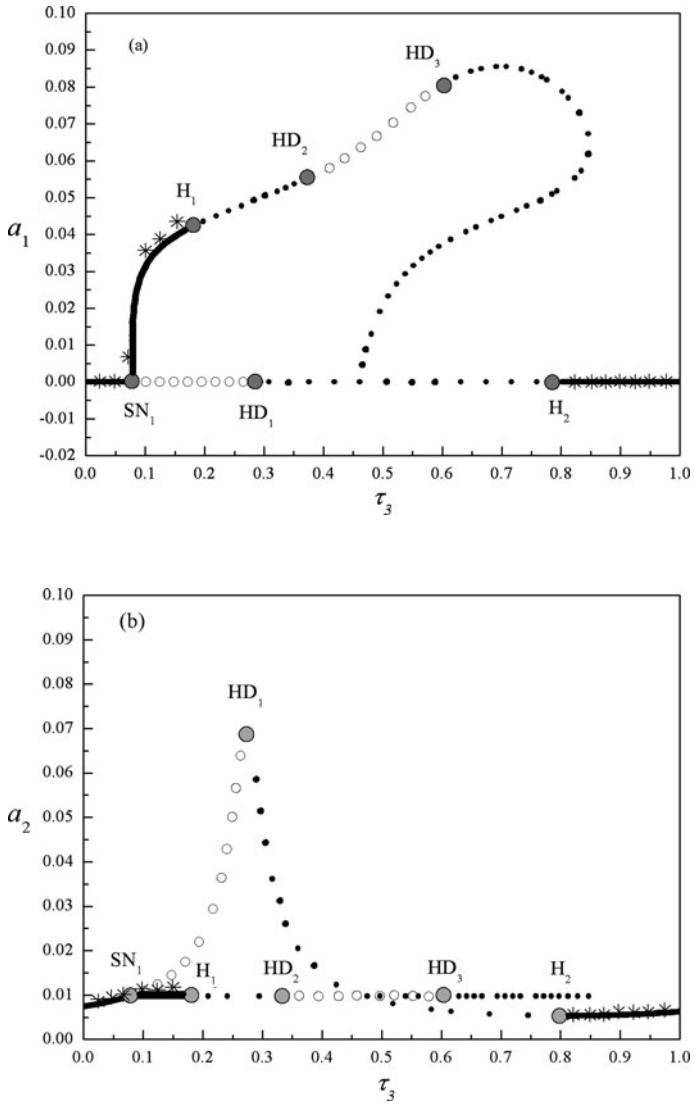

Fig. 2 Amplitude–delay (τ_3) response curve corresponding to Fig. 1(a) for $\tau_1 = \tau_2 = 0.5$

lution is stable if and only if the real parts of all eigenvalues are negative and unstable if positive. Following the Routh–Hurwitz criterion, the necessary and sufficient conditions are given by

$$\delta_1 > 0, \qquad \delta_1\delta_2 - \delta_3 > 0,$$
$$\delta_3(\delta_1\delta_2 - \delta_3) - \delta_1^2\delta_4 > 0, \qquad \delta_4 > 0. \tag{53}$$

Thus, saddle-node bifurcation may happen when

$$\delta_4 = 0, \tag{54}$$

and Hopf bifurcation occurs in the system if

$$\delta_1\delta_3 > 0, \qquad \delta_3(\delta_1\delta_2 - \delta_3) - \delta_1^2\delta_4 = 0. \tag{55}$$

6 Effect of time delays on saturation control

For a $16.53'' \times 2.5'' \times 0.0502''$ stainless-steel beam, Pai and Schultz [12] designed a saturation controller without time delay for suppressing its first-mode steady-state vibration. In that experimental setup, the first natural frequency ω_2 and modal damping ratio ξ_2 of the beam with four integrated PZT patches were obtained using modal testing at $\omega_2 = 5.85000$ Hz and $\xi_2 = 0.0025$. The measured density was $0.286100 b/in^3$ and the Young's modulus was derived to be 2.80000×10^7 psi by matching the measured first natural frequency with the theoretical one. u_1 and u_2 represent, respectively, the controller volt-

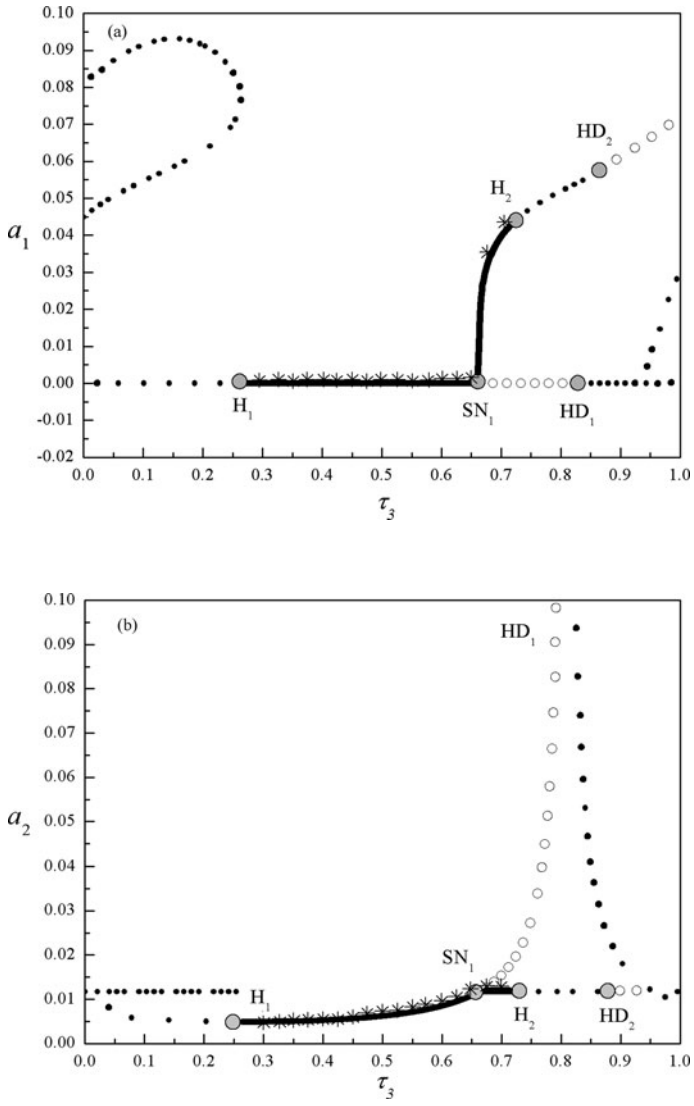

Fig. 3 Amplitude–delay (τ_3) response curve corresponding to Fig. 1(b) for $\tau_1 = \tau_2 = 0.5$

age and the sensor voltage inside the DS1102 controller, shown in Fig. 1 of [12]. g_1 and g_2 are the gains used in the DS1102 controller and f is the input voltage amplitude to the excitation PZT actuator. The damping ratio ξ_1 of the controller was set to zero to reduce a_2 in (40) and (41). The other parameters were derived in [12] using numerical simulation where $g_1 = 50.0$, $g_2 = 17.5323$, $f = 0.06754$, $g_3 = 0.10$ or $g_3 = -0.10$.

The theoretical study on vibration suppression using saturation control method was discussed in Pai and Schultz [12] without considering the effect of time delays. For the case of $\omega_1 = \omega_2/2$ (i.e., $\sigma_1 = 0$) and $\tau_1 = \tau_2 = \tau_3 = 0$, the effective frequency bandwidth of the saturation control can be obtained from (40) and (41), when $-0.493697 < \sigma_2 < 0.493697$ for $g_3 = 0.10$ and $-0.519015 < \sigma_2 < 0.519015$ for $g_3 = -0.10$. For τ_1, τ_2, $\tau_3 \neq 0$, the equilibrium solution can be obtained by setting $p_1' = q_1' = p_2' = q_2' = 0$ in (47)–(50) and using $a_i = \sqrt{p_i^2 + q_i^2}$ $(i = 1, 2)$. We note that the vibration of the controlled system can be saturated if and only if there are at least two stable equilibrium solutions in the system. To illustrate the fact that the delay may widen the effective frequency bandwidth of the saturation control, we choose $\sigma_2 = 0.5$ for $g_3 = 0.10$ and $\sigma_2 = 0.6$ for $g_3 = -0.10$ at which the saturation control is invalid for the system without delays. Using the

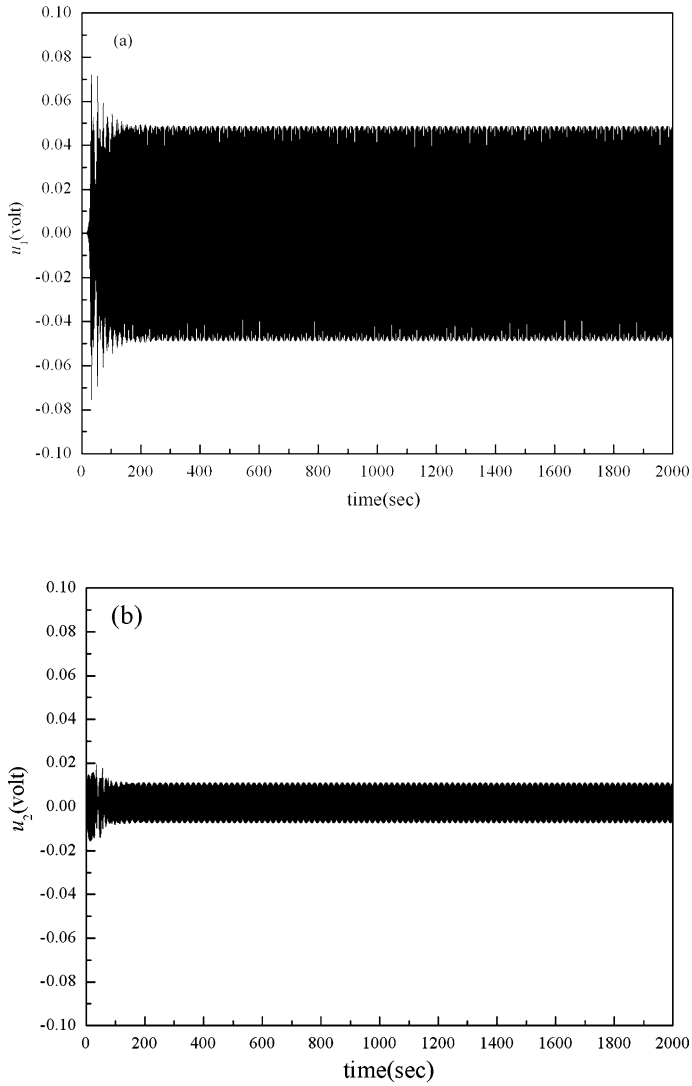

Fig. 4 Response of the controlled system in the range of saturation control when $\tau_3 = 0.15$

conditions of the saturation control together with (54) and (55), we may easily obtain the valid range of the saturation control in terms of τ_1, τ_2 and τ_3. Figure 1 shows the valid regions of the saturation control where $\tau_1 = \tau_2$, $H_{(\cdot)}$ and $SN_{(\cdot)}$ denote the Hopf and saddle-node bifurcation points, respectively. The single-mode motion occurs in range (I). The saturation control can be realized in range (II). Non-periodic motions are located in range (III). The existence of range (II) in Fig. 1 shows that, even through the saturation control without time delays fails for a specific frequency, appropriate delay values may be chosen so as to bring the system back to the saturation control. Thus, the effective frequency bandwidth can be widened. To understand the details displayed in Fig. 1, we investigate the amplitude–delay (τ_3) response curves for $\tau_1 = \tau_2 = 0.5$ in Figs. 2 and 3 which correspond to (a) and (b) in Fig. 1. Here, $HD_{(\cdot)}$ are the boundary points to distinguish those unstable foci from other unstable equilibria. The solid line, dot with black and dot with blank represent stable solutions, unstable foci and other unstable solutions predicted from (46)–(55), respectively.

It follows from Fig. 1 that the system is tuned into the range of the saturation control when τ_3 is between SN_1 and H_1. Correspondingly, the system has two equilibrium solutions, E_1 and E_3. Within this range, the amplitude of the controller a_1 increases with τ_3.

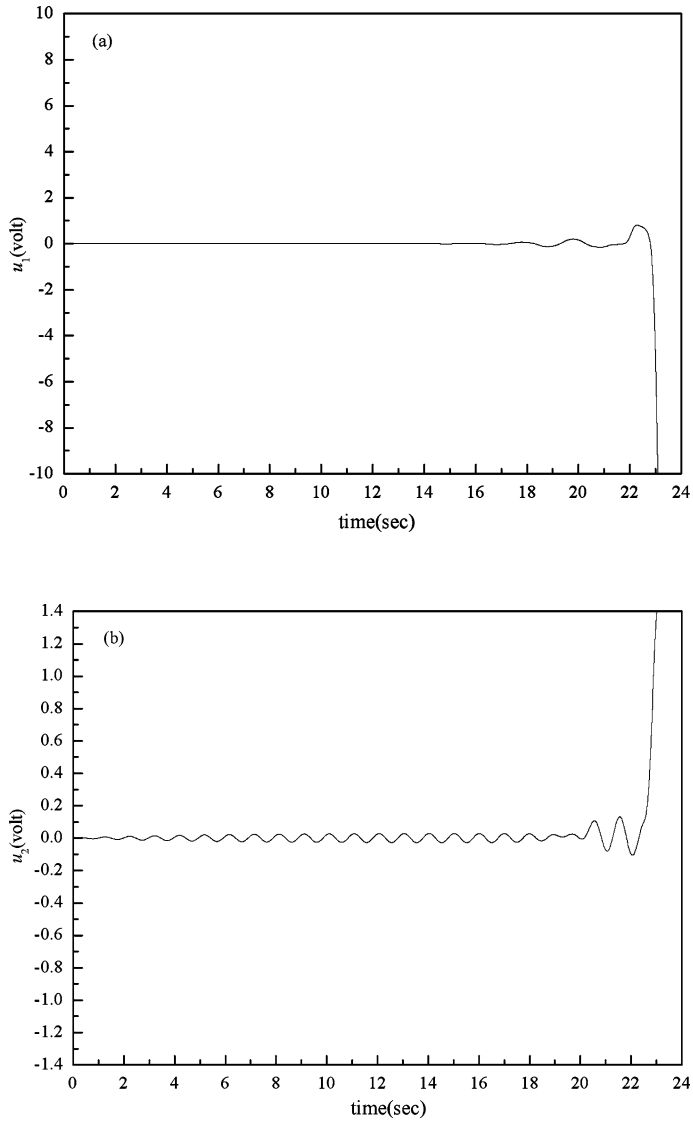

Fig. 5 Response of the controlled system in the range of unstable control when $\tau_3 = 0.2$

This shows that the energy added is absorbed by the controller so that the vibration of the beam is saturated. In Fig. 2(b), the amplitude of the beam a_2 is constant when τ_3 is between SN_1 and H_1. However, when a_1 reaches the value at H_1, the periodic solution loses its stability in a Hopf bifurcation. Then, complex motions emerge in the system and the saturation control for the vibration of the beam becomes invalid. The system is still in a single-mode motion when τ_3 is before SN_1 or after H_2. However, as predicted from the theoretical analysis, the system has only one equilibrium solution E_1 in these two intervals. The saturation control cannot be realized since the amplitude of the beam increases linearly with the excitation. A similar phenomenon is also observed in Fig. 3. The effective frequency bandwidth of the saturation control can be calculated from (40) and (41) for a fixed value of τ_3. For instance, for $g_3 = 0.10$, the effective frequency bandwidth of the saturation control is $-0.337235 < \sigma_2 < 0.665978$ when $\tau_3 = 0.15$. For $g_3 = -0.10$, the effective frequency bandwidth is $-0.395586 < \sigma_2 < 0.704506$ when $\tau_3 = 0.7$. Comparing with (1) and (2) where $\tau_i = 0$ $(i = 1, 2, 3)$, the effective frequency bandwidths are wider in both cases.

To verify the above analytical prediction, we compute the solution of (3) and (4) numerically under

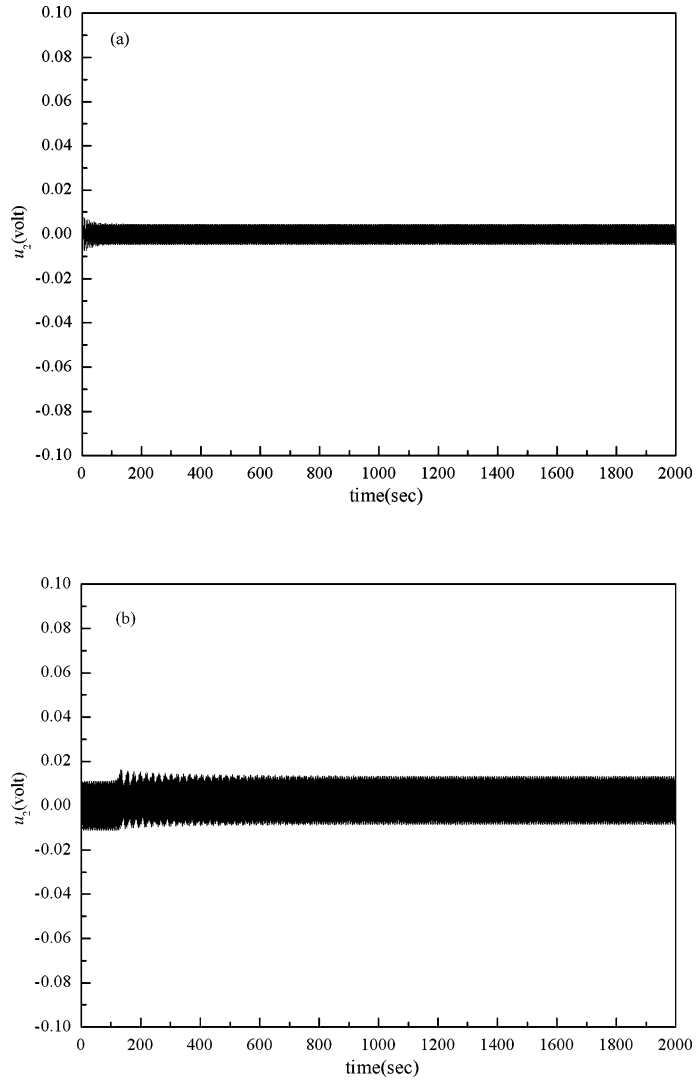

Fig. 6 Response of the controlled beam for different values of τ_3: (**a**) $\tau_3 = 0.3$, (**b**) $\tau_3 = 0.6$

the initial conditions given by $u_1(0) = u_2(0) = 10^{-4}$, $\dot{u}_1(0) = \dot{u}_2(0) = 10^{-4}$, $u_1(t) = u_2(t) = 0$, $\dot{u}_1(t) = \dot{u}_2(t) = 0$ for $t \in [-\tau, 0)$. All the numerical results are labeled with the star symbol in Figs. 2 and 3. For instance, the analytical prediction in Figs. 2(a) and 2(b) shows that the saturation control is achieved for $\tau_3 = 0.15$, but fails when $\tau_3 = 0.2$. The numerical simulation validates such predictions both quantitatively and qualitatively, as shown in Figs. 4 and 5. Therefore, the numerical simulation is in agreement with the analytical prediction.

Next, we investigate the effect of delays on the dynamics of the controlled beam when the saturation control is invalid. In fact, an appropriate choice of τ_3 may still be used for vibration suppression of the controlled beam even when τ_3 is between H_1 and H_2 in Fig. 2. Based on (3) and (4), Figs. 6(a) and 6(b) show numerically the response of the controlled beam for $\tau_3 = 0.3$ and $\tau_3 = 0.6$, respectively. We note that the amplitude of the beam is around 0.005 in Fig. 6(a) and 0.01 in Fig. 6(b). It indicates that a minimal value of the amplitude in the controlled beam can be achieved by tuning τ_3 even if the system is in a single-mode motion. This suggests that τ_3 may be considered as a controlling parameter for the amplitude of the controlled beam.

All results mentioned above indicate that the delays have positive effect on either the saturation control or the vibration suppression. However, lager value of the delays may also cause negative effect on the

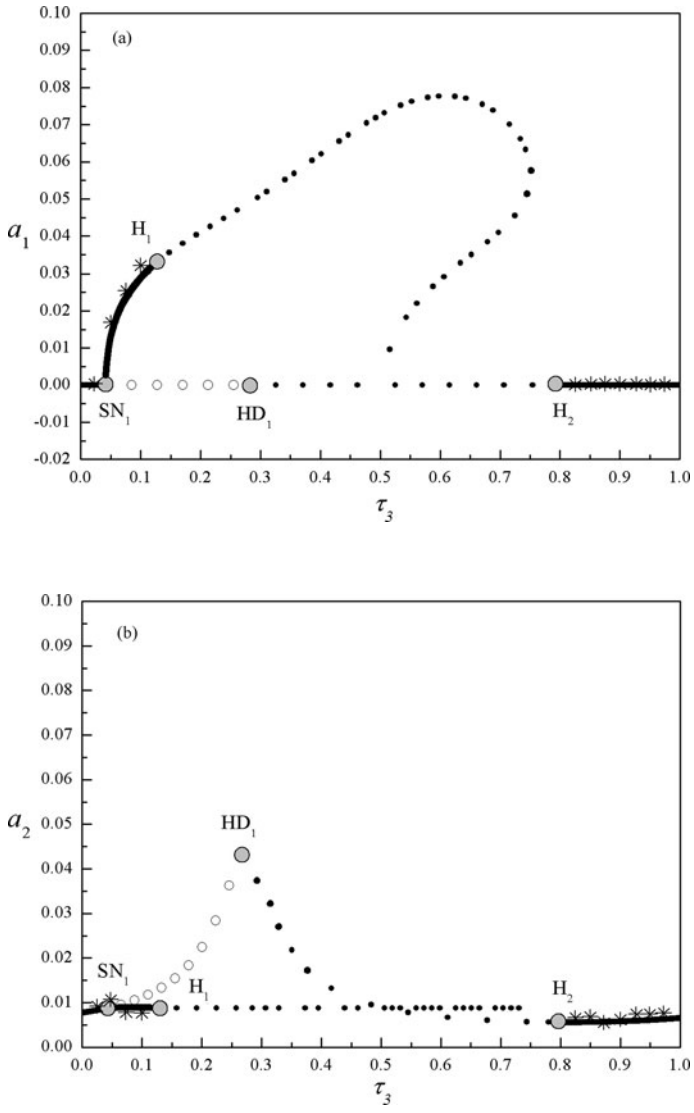

Fig. 7 Amplitude–delay (τ_3) response curve for $\tau_1 = \tau_2 = 1$, $g_3 = 0.10$ and $\sigma_2 = 0.45$

controlled system [11]. The vibration of the controlled beam can be saturated at $\sigma_2 = 0.45$ for both $g_3 = 0.10$ and $g_3 = -0.10$ when $\tau_1 = \tau_2 = \tau_3 = 0$. However, when $\tau_1 = \tau_2 = 1$, the saturation control is invalid even for $\tau_3 = 0$ (see Fig. 7 for $g_3 = 0.10$ and Fig. 8 for $g_3 = -0.10$). Although an increase in τ_3 ensures that the vibration will return to the saturation state, the effective frequency bandwidth of the saturation control may shrink at the same time. For instance, for $g_3 = -0.10$, $\tau_3 = 0.6$ is in the valid range of the saturation control as shown in Fig. 8. However, the effective frequency bandwidth is $-0.367623 < \sigma_2 < 0.477101$ which is narrower than that without the time delays. Therefore, large delays may lead to shrinkage in the effective frequency bandwidth of the saturation control.

7 Conclusion and discussion

The saturation phenomenon is utilized to control the amplitude of the vibration of a stainless-steel beam by using a second-order controller with three delays. This paper focuses on the effect of these delays on the saturation control strategy both qualitatively and quantitatively. The results are summarized as follows.

(1) The approximate analytical solutions of the delayed system are obtained by the method of multi-

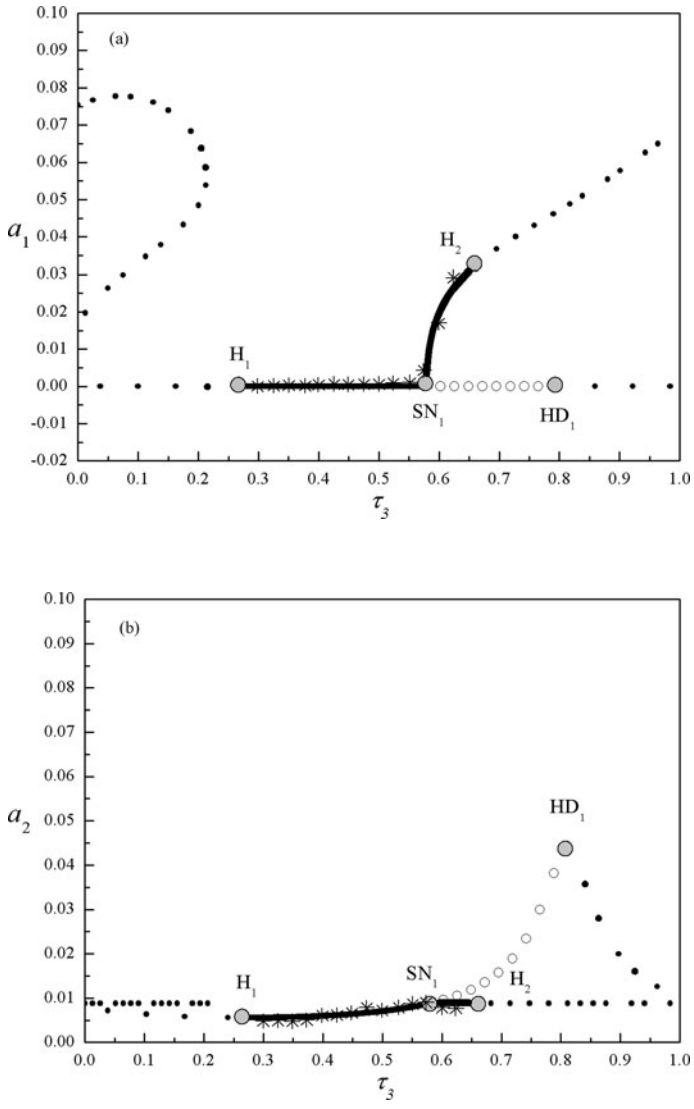

Fig. 8 Amplitude–delay (τ_3) response curve for $\tau_1 = \tau_2 = 1$, $g_3 = -0.10$ and $\sigma_2 = 0.45$

ple scales. The analytical predictions are in agreement with those obtained from numerical simulation both quantitatively and qualitatively.

(2) The range of the saturation control can be changed using the time delays. The effective frequency bandwidth of the saturation control may either shrink or be widened. It depends on the choice of the time delays.

(3) A frequency in the single-mode motion may be tuned into the range of the saturation control if appropriate values of time delays are chosen.

(4) A frequency in the saturation control may be tuned into the single-mode motion when the time delay arisen from self-feedback signal is used as the control parameter.

(5) Time delays may be considered as controlling parameters for suppressing the vibration of the controlled beam.

Finally, we give a brief discussion to end the paper. Figure 1 shows various stability regions in the controlled system for different g_3 values in the linear self-feedback gain. Such results may somehow tie in with the linear stability analysis of the system when the gain and the delay in the linear feedback $-2g_3\omega_2\dot{u}_2(t-\tau)$ are considered as variable parameters. Usually, a linear stability analysis of the delayed system can help to

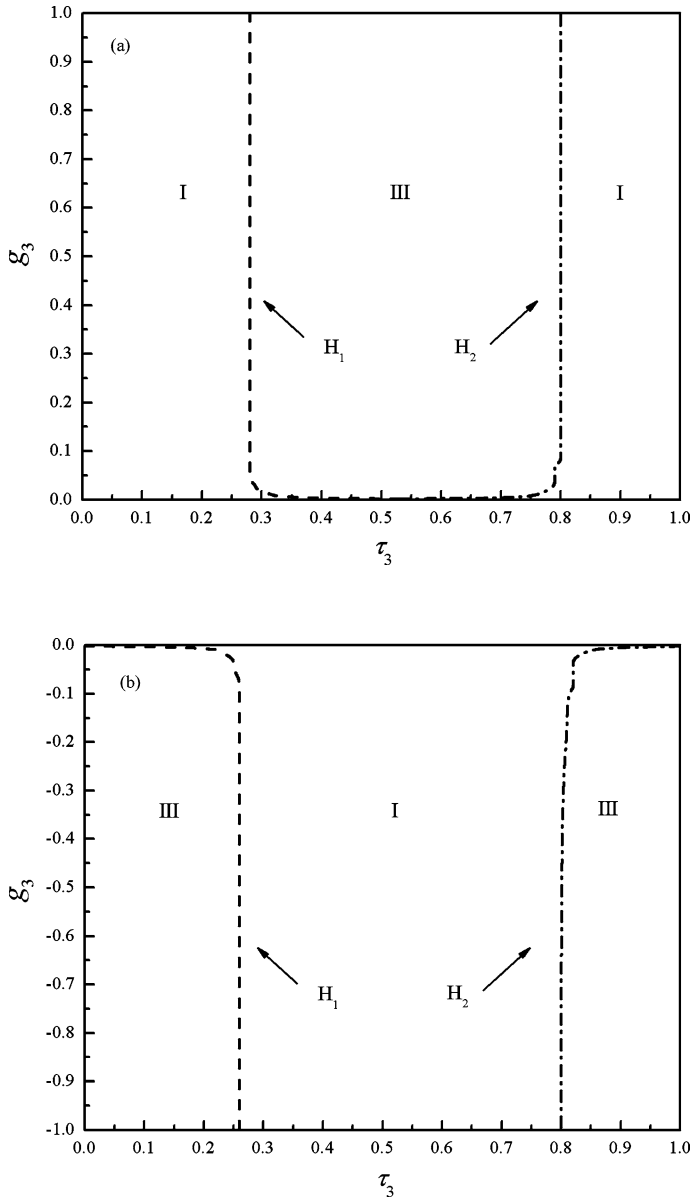

Fig. 9 Stability regions in the linearized system corresponding to (3) and (4) for (**a**) $\sigma_2 = 0.5$, (**b**) $\sigma_2 = 0.6$, where region (I) represents the stable periodic solution of the beam and region (III) the complex motions

gain a deeper insight into the problem, especially when large delays are utilized. Figure 9 shows the stability regions of the solution of u_2 for the linearized system corresponding to (3) and (4), where the parameters are the same as those in Fig. 1. It follows from Fig. 9 that the stable periodic solution of the beam can also occur in the system even for a large delay. This provides the possibility that a large delay can be utilized. Unfortunately, the saturation control is not achievable. This is because the linearized system corresponding to (3) and (4) consists of two independent subsystems so that the controller has no effect on the beam. When the controller is coupled onto the beam, the regions of the saturation control can be found in the parameter plane as shown in Fig. 10. This suggests that the saturating region occurs in the system not only for a small delay but also for a large delay, which exhibits an attractive feature on the delayed control.

Acknowledgements This work was supported by the NNSF of China under Grant No. 10532050, the National Outstand-

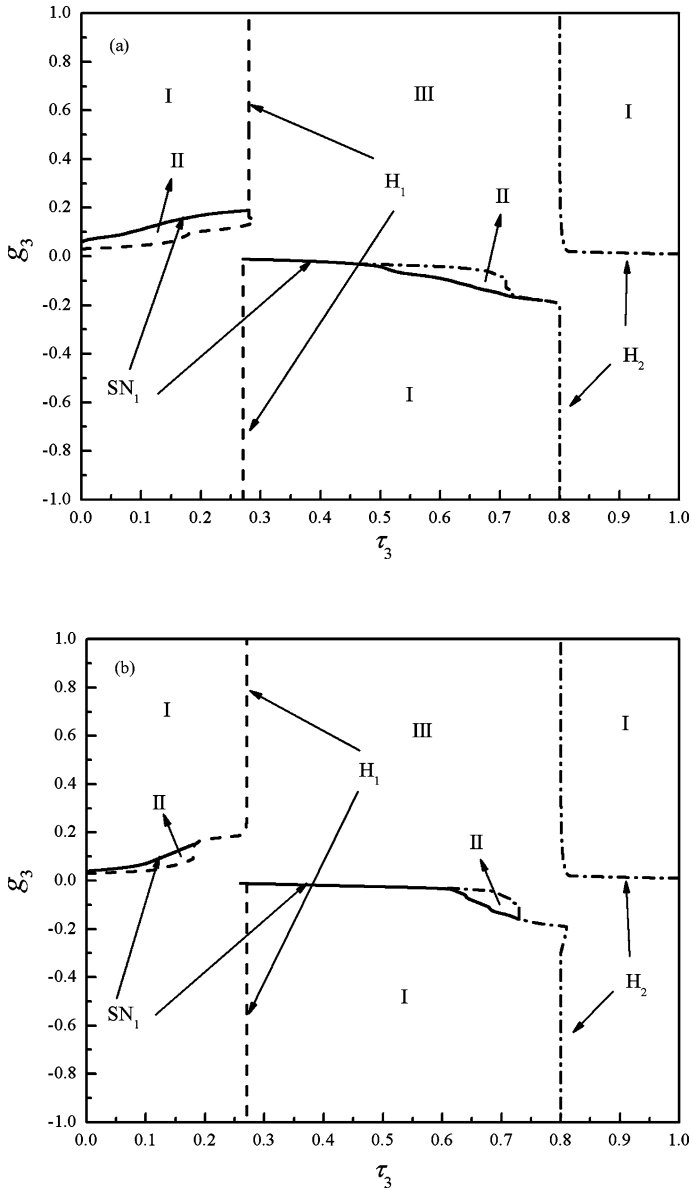

Fig. 10 Analytical prediction for single mode (I), saturation (II) and complex vibrations (III) in (3) and (4) when $\tau_1 = \tau_2 = 0.5$. Values of the other parameters are the same as those in Fig. 1: (**a**) $\sigma_2 = 0.5$, (**b**) $\sigma_2 = 0.6$

ing Young Funds of China under Grant No. 10625211 and the Hong Kong Research Grants Council under CERG Grant (Cityu 1007/05E).

References

1. Haxton, R., Barr, A.: The autoparametric vibration absorber. J. Eng. Ind. **94**, 119–225 (1972)
2. Nayfeh, A.H., Mook, D.T., Marshall, L.R.: Nonlinear coupling of pitch and roll modes in ship motion. J. Hydronaut. **7**, 145–152 (1973)
3. Haddow, A.G., Barr, A.D.S., Mook, D.T.: Theoretical and experimental study of modal interaction in a two degree-of-freedom structure. J. Sound Vib. **97**(3), 451–473 (1984)
4. Nayfeh, A.H., Zavodney, L.D.: Experimental observation of amplitude- and phase-modulated responses of two internally coupled oscillators to a harmonic excitation. ASME J. Appl. Mech. **55**, 706–710 (1988)
5. Nayfeh, A.H., Balachandran, B.: Modal interactions in dynamical and structural systems. ASME Appl. Mech. Rev. **42**(11), 175–201 (1989)
6. Oueini, S.S., Nayfeh, A.H., Golnaraghi, M.F.: A theoretical and experimental implementation of a control method based on saturation. Nonlinear Dyn. **13**, 189–202 (1997)

7. Oueini, S.S., Golnaraghi, M.F.: Experimental implementation of the internal resonance control strategy. J. Sound Vib. **191**, 377–396 (1996)
8. Oueini, S.S., Nayfeh, A.H.: Analysis and application of a nonlinear vibration absorber. J. Vib. Control **6**(7), 999–1016 (2000)
9. Pai, P.F., Wen, B., Naser, A.S., Schultz, M.J.: Structural vibration control using PZT patches and non-linear phenomena. J. Sound Vib. **215**, 273–296 (1998)
10. Pratt, J.R., Oueini, S.S., Nayfeh, A.H.: A Terfenol-D nonlinear vibration absorber. J. Intell. Mater. Syst. Struct. **10**, 29–35 (1999)
11. Pai, P.F., Wen, B., Naser, A.S., Schultz, M.J.: Nonlinear vibration suppression of cantilever beams using bi-moments induced by PZT actuators. In: Proceedings of 38th AIAA Structures, Structural Dynamics & Materials Conference, Hyatt Orlando, FL, pp. 1789–1795 (1997)
12. Pai, P.F., Schultz, M.J.: A refined nonlinear vibration absorber. Int. J. Mech. Sci. **42**, 537–560 (2000)
13. Saguranrum, S., Kunz, D.L., Omar, H.M.: Numerical simulations of cantilever beam response with saturation control and full modal coupling. Comput. Struct. **81**, 1499–1510 (2003)
14. Shoeybi, M., Ghorashi, M.: Control of a nonlinear system using the saturation phenomenon. Nonlinear Dyn. **42**, 113–126 (2005)
15. Shoeybi, M., Ghorashi, M.: Nonlinear vibration control of a system with dry friction and viscous damping using the saturation phenomenon. Nonlinear Dyn. **45**, 249–272 (2006)
16. Li, J., Hua, H.X., Shen, R.Y.: Saturation-based active absorber for a non-linear plant to a principal external excitation. Mech. Syst. Signal Process. **21**, 1489–1498 (2007)
17. Chu, S.Y., Soong, T.T., Lin, C.C., Chen, Y.Z.: Time-delay effect and compensation on direct output feedback controlled mass damper system. Earthquake Eng. Struct. Dyn. **32**, 121–137 (2002)
18. Yang, B., Mote, C.D.: Noncollocated control of a damped string using time delay. J. Dyn. Syst. Meas. Control **114**(4), 736–740 (1992)
19. Abdel, M.M., Roorda, J.: Time delay compensation in active damping of structures. J. Eng. Mech. **117**(11), 2549–2570 (1991)
20. Rodellar, J., Chung, L.L., Soong, T.T., Reinhorn, A.M.: Experimental digital control of structures. J. Eng. Mech. **115**, 1245–1261 (1989)
21. Xu, J., Chung, K.W.: Effects of time delayed position feedback on a van der Pol–Duffing oscillator. Physica D **180** (1–2), 17–39 (2003)
22. Guan, Y.H., Lim, T.C., Shepard, W.S.: Experimental study on active vibration control of a gearbox system. J. Sound Vib. **282**, 713–733 (2005)
23. Hu, H.Y., Dowell, E.H., Virgin, L.: Resonances of a harmonically forced Duffing oscillator with time delay state feedback. Nonlinear Dyn. **45**, 249–272 (2006)
24. Xu, J., Yu, P.: Delay-induced bifurcations in a nonautonomous system with delayed velocity feedbacks. Int. J. Bifurc. Chaos **14**(8), 2777–2798 (2004)
25. Olgac, N., McFarland, D., Holm-Hansen, B.T.: Position feedback-induced resonance: the delayed resonator. In: ASME Winter Annu. Meet., vol. 38, pp. 113–119 (1992)
26. Filipovic, D., Olgac, N.: Delayed resonator with speed feedback—design and performance analysis. Mechatronics **12**(3), 393–413 (2002)
27. Zhao, Y.Y., Xu, J.: Effects of delayed feedback control on nonlinear vibration absorber system. J. Sound Vib. **308**, 212–230 (2007)
28. Wirkus, S., Rand, R.: The dynamics of two coupled van der Pol oscillators with delay coupling. Nonlinear Dyn. **30**, 205–221 (2002)